Investigation on a Hardware Simplified Static Synchronous Compensator

Tsao-Tsung Ma, *Member, IEEE*

***Abstract*—Inverter based flexible ac transmission system (FACTS) devices have been expected to play important roles in operating and controlling modern power systems, in which a number of potential concepts, e.g. distributed generation and micro-grid are implemented. FACTS devices can be divided into series-type and shunt-type controllers based on their connection means with the system. As one of the shunt-type FACTS devices, the static synchronous compensator (STATCOM) is the most versatile and powerful FACTS device that can provide effective means for controlling reactive power flow and improving the voltage stability of power networks. However, the STATCOM circuitry has complex and coupled system dynamics which require advanced controllers to achieve satisfactory performances. This paper presents the investigation of a hardware simplified STATCOM in providing satisfactory performances in performing various reactive power flow control functions during steady-state and dynamic operations of power systems. For comparative purposes, two topologies, i.e. 2-leg 4-switch (2L-4S) and 3-leg 6-switch (3L-6S) based STATCOM are investigated in this study. Mathematical models and simulation studies carried out in the Matlab/Simulink environment are firstly described. Typical results are then presented to verify the feasibility of the 2L-4S STATCOM and the effectiveness of the proposed controllers.**

***Index Terms*—Three-phase inverter, flexible ac transmission systems (FACTS), static synchronous compensator (STATCOM), space vector pulse width modulation (SVPWM)**

I. Introduction

In recent years, concepts concerning distributed and renewable generation, micro-grid, together with the optimal real-time system management, are being promoted to reduce the use of central fossil fired power plant, increase the reliability and efficiency in delivery of energy and reduce emissions. It is envisaged that flexible ac transmission systems (FACTS) devices or controllers are going to play a critical role in operating the new type of power systems under such a complex operating environment [1]-[5]. The basic concept drawn from the flexible ac transmission systems (FACTS) terminology emerges as a remedy to release the extremely transmission system tension. It needs the aid of modern power electronics and advanced control techniques to successfully replace the conventional mechanical controlled apparatuses in systems. By doing so, FACTS technology has been expected to offer a number of advantages, i.e. to bring the transfer capability of transmission line approaching its thermal limit without violating the stability criteria, to re-assign power flows at will and on a real-time basis so as to facilitate an ideal electricity market and to increase the riding through capability when critical faults are encountered. Besides, FACTS devices can also enhance the operating flexibility of the power system with their fast control characteristics and continuous compensating capabilities. Of the known FACTS devices, the STATCOM being a new generation of reactive power compensating devices has been widely used in various power system control [5]-[17]. From the hardware point of view, a STATCOM is similar to the shunt branch of the unified power flow controller (UPFC) and can be controlled to provide concurrent real and reactive compensations with an external electric energy source adding to its internal dc bus. In the literature, a number of feasible hardware configurations have been proposed for the STATCOM to perform various reactive power and voltage control functions in power systems embedded with distributed generators; however, most of them are designed on a 3-leg 6-switch (3L-6S) structure operated either by SPWM or multi-module and multi-level techniques [18]-[22]. To achieve a cost-effective design without sacrificing the control performances some possible topologies with advanced controllers and fast-response features are still call for investigations.

This paper presents the feature study of a two-leg four-switch (2L-4S) STATCOM to provide satisfactory performances in performing various reactive power flow control functions during steady-state and transient operations of power systems. To verify the overall performance of the hardware simplified STATCOM, two topologies with three switching techniques, i.e. SPWM, voltage hysteresis and SVPWM, have been investigated in this paper. Comprehensive simulation studies are carried out in the Matlab/Simulink environment and results of various power flow control examples are presented to show the successful design of the 2L-4S STATCOM and the effectiveness of the proposed control strategy.

II. STATCOM Principles and Its Controllers

A. STATCOM Review

In a conventional STATCOM system, the internal 3 phase inverter normally constructed by a 3-leg and 6-switch configuration provides the main control functions via connecting its output voltage with a controllable magnitude and phase angle in shunt with the compensated power system through a transformer. In this paper, a simple three-phase converter constituted by 2-leg and 4-switch is adopted to perform both the reactive power and voltage compensation tasks [23]-[25]. This arrangement can provide an alternative topology for STATCOM with lower system cost; however, the related controllers must be properly designed to achieve a satisfactory performance. Fig. 1 shows a simple test power

Manuscript received May 18, 2011; revised May 25, 2011. This work was supported in part by the National Science Council of Taiwan, R.O.C. through: NSC 99-2221-E-239-038.

Tsao-Tsung Ma is with the Dept. of Electrical Engineering, CEECS, National United University, Taiwan, R.O.C. (phone: +886-37-381369; fax: +886-37-327887; e-mail: tonyma@nuu.edu.tw; tonyma@ieee.org).

system model with the proposed 2-leg and 4-switch STATCOM configuration. As shown in Fig. 1, the STATCOM is connected to a distribution system at the load terminal. The overall system is represented by a three-phase voltage source behind the series *R-L* elements in each phase. In a STATCOM system, the voltage acts essentially as a controllable synchronous ac voltage source. In addition to the dc voltage regulator, the three-phase inverter can independently generate or absorb controllable reactive power as desired and thereby provides independent shunt reactive compensation for the system. It is important to note that if a dc energy source can be added to the STATCOM the control of real and reactive power on the connected point of transmission line can be achieved by adjusting the voltage with an appropriate magnitude and angle of the inverter. In this study, the output reactive power of a STATCOM is controlled by the magnitude of q-axis current component of the proposed 2L-4S STATCOM.

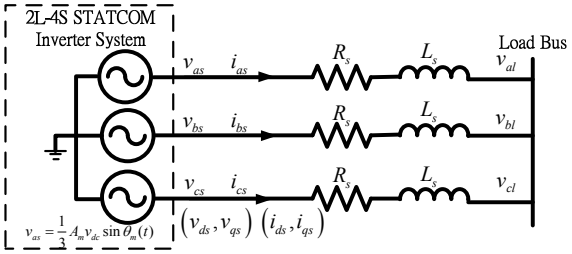

Fig. 1. Schematic representation of the test power system with a 2L-4S STATCOM.

B. STATCOM Mathematical Model

From Fig. 1, the ac-side voltage equations of the STATCOM model can be expressed as:

$$v_{abcs} = R_S i_{abcs} + L_s p(i_{abcs}) + v_{abcl} \tag{1}$$

The *P* in the above equation is a derivative operator. In (1), $R_S = diag\{R_s, R_s, R_s\}$, $L_S = diag\{L_s, L_s, L_s\}$, and

$$v_{abcs} = \begin{bmatrix} V_{as} & V_{bs} & V_{cs} \end{bmatrix}^T \tag{2}$$

$$i_{abcs} = \begin{bmatrix} i_{as} & i_{bs} & i_{cs} \end{bmatrix}^T \tag{3}$$

$$v_{abcl} = \begin{bmatrix} V_{al} & V_{bl} & V_{cl} \end{bmatrix}^T \tag{4}$$

Considering only the fundamental components of the switching functions of the converter switches, the STATCOM terminal voltages can be expressed as follows:

$$\begin{bmatrix} v_{as}(t) \\ v_{bs}(t) \\ v_{cs}(t) \end{bmatrix} = \frac{1}{\sqrt{3}} A_m v_{dc} \begin{bmatrix} \sin\theta_m(t) \\ \sin(\theta_m(t) - \frac{2\pi}{3}) \\ \sin(\theta_m(t) + \frac{2\pi}{3}) \end{bmatrix} \tag{5}$$

where, $\theta_m(t) = \omega t + \alpha_m$. A_m and α_m are respectively the amplitude and angle modulation indices. ω is the system frequency, and v_{dc} is the dc bus voltage of the STATCOM inverter. Since the dynamic model of an electrical power system is conventionally developed in a d-q frame, it is desirable to obtain the model of STATCOM in the utility d-q frame. To transfer the *abc* variables to a d-q frame, a transformation matrix is selected such that the voltage and current components of STATCOM are proportional to its real and reactive power components respectively. Thus, the control of each current component regulating the corresponding power components can be achieved. The STATCOM variables in the *abc* frame can be transferred to the d-q frame by the Clark transformation.

$$f_{qdos} = K f_{abcs} \tag{6}$$

The transformation matrix *K* is defined as

$$K = \frac{2}{3} \begin{bmatrix} \cos\theta_s & \cos\left(\theta_s - \frac{2\pi}{3}\right) & \cos\left(\theta_s + \frac{2\pi}{3}\right) \\ \sin\theta_s & \sin\left(\theta_s - \frac{2\pi}{3}\right) & \sin\left(\theta_s + \frac{2\pi}{3}\right) \\ \frac{1}{2} & \frac{1}{2} & \frac{1}{2} \end{bmatrix} \tag{7}$$

Substituting *abc* variables from (1) to (5) into (6), the voltage equations (8) of the STATCOM in the d-q frame are obtained using (7):

$$\frac{1}{\sqrt{3}} A_m v_{dc} \begin{bmatrix} \sin(\alpha_m - \alpha) \\ \cos(\alpha_m - \alpha) \\ 0 \end{bmatrix} = R_S i_{dqos} + L_s p(i_{dqos}) + \omega \begin{bmatrix} 0 & 1 & 0 \\ -1 & 0 & 0 \\ 0 & 0 & 0 \end{bmatrix} L_s i_{dqos} + v_{ml} \begin{bmatrix} 0 \\ 1 \\ 0 \end{bmatrix} \tag{8}$$

The V_{ml} is the amplitude of load terminal voltage. For the dc-side circuit of the STATCOM, we have

$$p\left(\frac{v_{dc}}{2}\right) = \frac{1}{C}\left(i_{dc}\right) \tag{9}$$

and the dc-side current can be mathematically expressed as

$$i_{dc} = \frac{-1}{\sqrt{3}} A_m \begin{bmatrix} i_{as} \sin(\theta_m) + i_{bs} \sin\left(\theta_m - \frac{2\pi}{3}\right) \\ + i_{cs} \sin\left(\theta_m + \frac{2\pi}{3}\right) \end{bmatrix} \quad (10)$$

Using abc variables from (10) and the transformation equation (6), the d-q model of the dc circuit can be obtained as (11).

$$p\left(\frac{v_{dc}}{2}\right) = \frac{-3}{2\sqrt{3}} \frac{A_m}{C} \begin{bmatrix} i_{qs} \sin(\alpha_m - \alpha) \\ + i_{ds} \cos(\alpha_m - \alpha) \end{bmatrix} \quad (11)$$

Under steady-state and balanced three phase conditions, the three phase active power and reactive power of the STATCOM may be expressed in terms of d-q quantities as (12) and (13), where the v and i are the peak values of phase voltage and phase current respectively, and θv and θi are the phase angles for phase voltage v_a and phase current i_a respectively.

$$P_{STATCOM} = \frac{3}{2}\left(v_q i_q + v_d i_d\right) \quad (12)$$

$$Q_{STATCOM} = \frac{3}{2}\left(v_q i_q - v_d i_d\right) \quad (13)$$

C. Voltage SVPWM Controllers for the Voltage Source Inverter

The modeling steps of a space vector pulse width modulation (SVPWM) algorithm are adopted from the author's previous work [21] and described again in this subsection. In practical operations, two feasible configurations are depicted in Fig. 2(a) and (b). The corresponding current paths are shown in Fig. 3 (a) to (h).

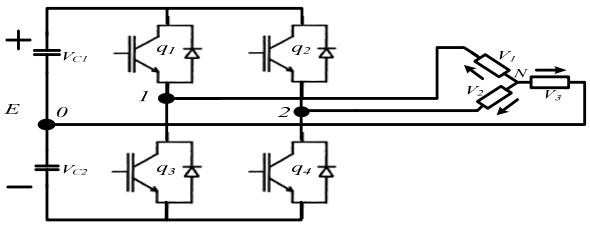

Fig. 2.(a) Topology structure of three-phase voltage source inverter(Y)

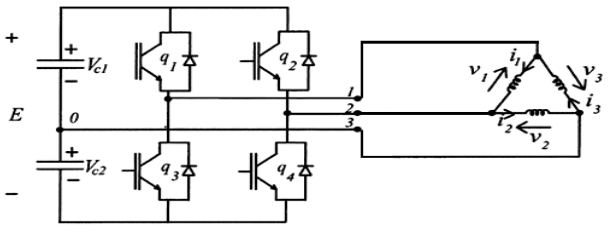

Fig. 2.(b) Topology structure of three-phase voltage source inverter(Delta)

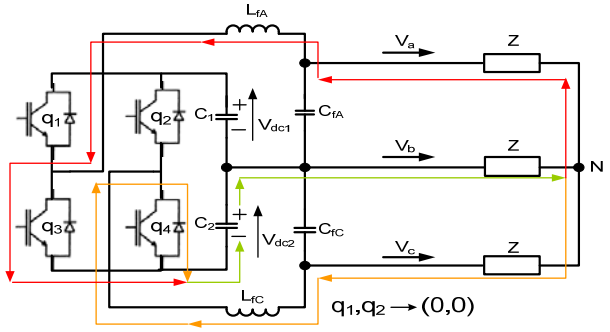

Fig. 3.(a) The current paths of three-phase voltage source inverter for Y-connection, at q1,q2=(0,0).

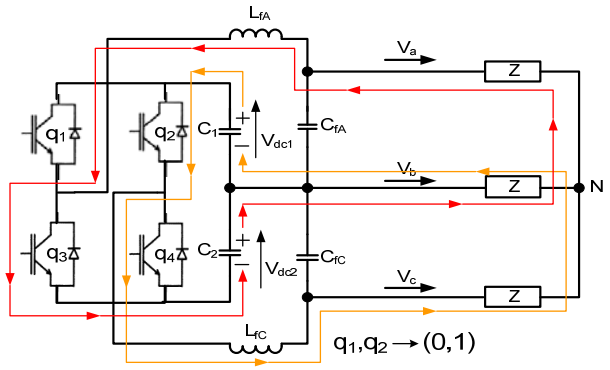

Fig. 3.(b) The current paths of three-phase voltage source inverter for Y-connection, at q1,q2=(0,1).

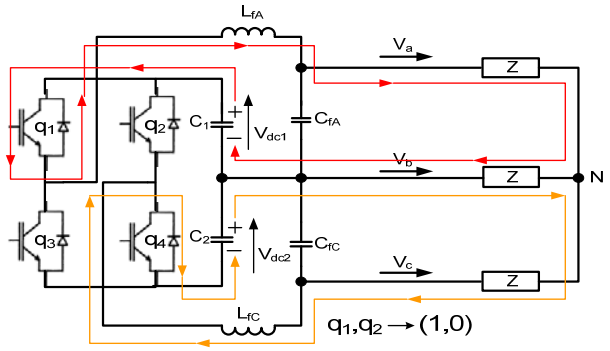

Fig. 3.(c) The current paths of three-phase voltage source inverter for Y-connection, at q1,q2=(1,0).

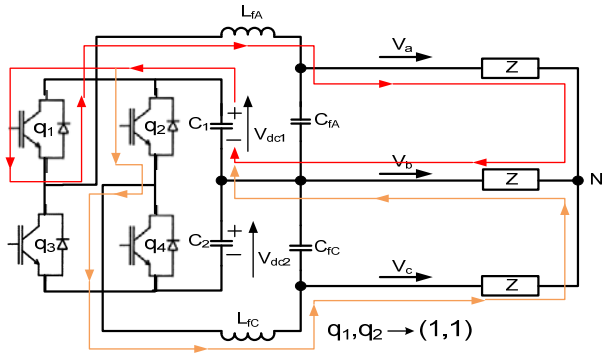

Fig. 3.(d) The current paths of three-phase voltage source inverter for Y-connection, at q1,q2=(1,1).

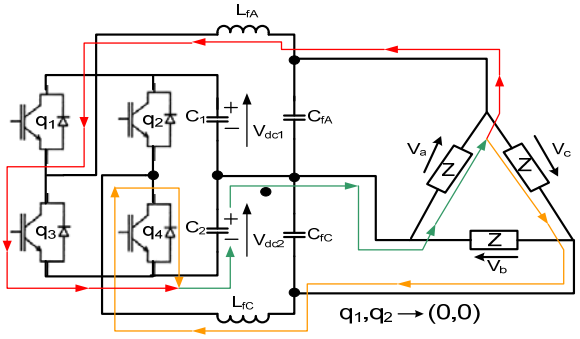

Fig. 3.(e) The current paths of three-phase voltage source inverter for Delta-connection, at q1,q2=(0,0).

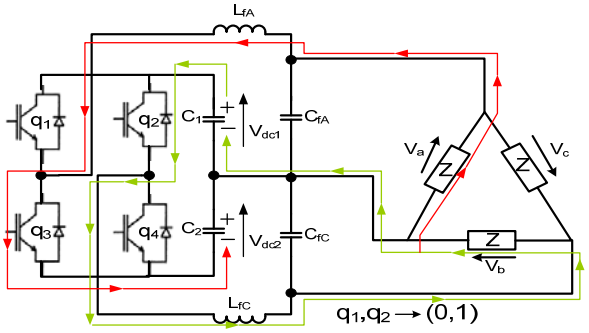

Fig. 3.(f) The current paths of three-phase voltage source inverter for Delta-connection, at q1,q2=(0,1).

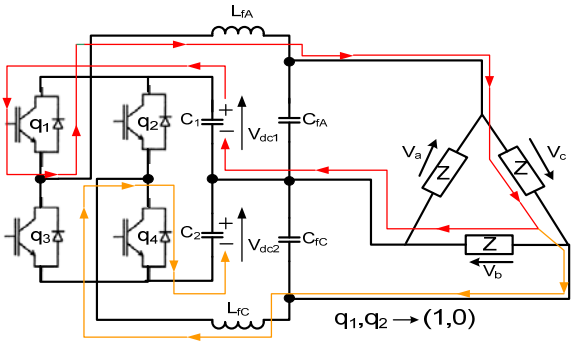

Fig. 3.(g) The current paths of three-phase voltage source inverter for Delta-connection, at q1,q2=(1,0).

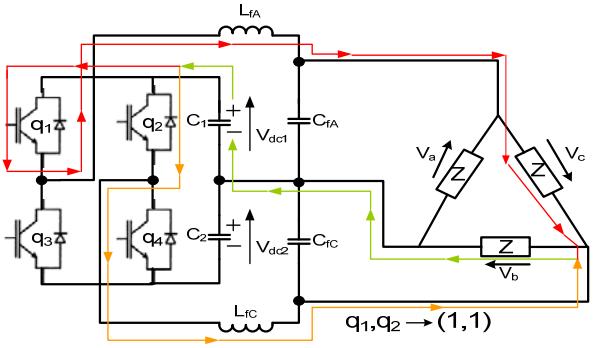

Fig. 3.(h) The current paths of three-phase voltage source inverter for Delta-connection, at q1,q2=(1,1).

In this paper, the derivations of control algorithms are based on the system setup shown in Fig. 2(b). Here, the switching status is represented by binary variables q_1 to q_4, which are set to "1" when the switch is closed and "0" when it is open. In addition, the switches in one inverter branch are controlled complementary, therefore:

$$q_1 + q_3 = 1 \tag{14}$$

$$q_2 + q_4 = 1 \tag{15}$$

Combinations of switching S1-S4 result in 4 general space vectors V_1 -V_4, as shown in Fig.4. The components $\alpha\beta$ of the voltage vectors are gained from *abc* voltages by using Clark's transformation.

The combinations of the states of the switches originate four different vectors and the related parameters in the αβ plane are given in Table 1 and 2. These vectors are phase shifted of $\pi/2$ from each other. Using the above vector definitions one may split the αβ plane into four (I to IV) sectors as shown in Fig. 4.

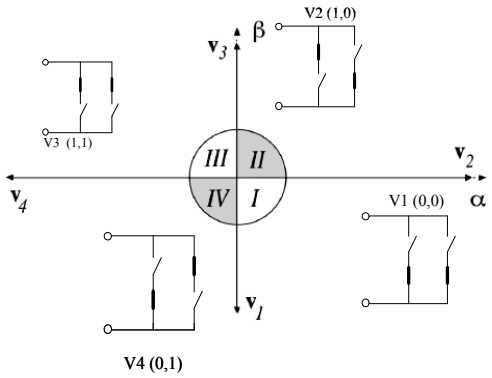

Fig. 4. Basic voltage space vectors for 2L-4S inverter

From Fig. 2(b), the following relations can be derived.

$$V_1 = V_{10} - V_{20}\ , V_2 = V_{20} - V_{30}$$

$$V_3 = V_{30} - V_{10}\ ,\ V_2 = -V_4$$

It follows that, V_1, V_2 and V_3 can be derived as follows:

$$V_{10} = (2q_1 - 1)\frac{V_{dc}}{2} \tag{16}$$

$$V_{20} = (2q_2 - 1)\frac{V_{dc}}{2} \tag{17}$$

$$V_{30} = 0 \tag{18}$$

$$\begin{aligned} V_1 &= (2q_1 - 1)\frac{V_{dc}}{2} - (2q_2 - 1)\frac{V_{dc}}{2} \\ &= q_1 V_{dc} - \frac{V_{dc}}{2} - q_2 V_{dc} + \frac{V_{dc}}{2} \\ &= q_1 V_{dc} - q_2 V_{dc} \end{aligned} \tag{19}$$

$$V_2 = (2q_2 - 1)\frac{V_{dc}}{2} \tag{20}$$

$$V_3 = -\left(2q_1 - 1\right)\frac{V_{dc}}{2} \tag{21}$$

Consequently, the voltage components, V_α, V_β can be obtained by performing the following Clark transformation.

$$\begin{bmatrix} V_\alpha \\ V_\beta \end{bmatrix} = \sqrt{\frac{2}{3}} \begin{bmatrix} 1 & -\frac{1}{2} & -\frac{1}{2} \\ 0 & \frac{\sqrt{3}}{2} & -\frac{\sqrt{3}}{2} \end{bmatrix} \begin{bmatrix} q_1 V_{dc} - q_2 V_{dc} \\ \left(2q_2 - 1\right)\frac{V_{dc}}{2} \\ -\left(2q_1 - 1\right)\frac{V_{dc}}{2} \end{bmatrix} \tag{22}$$

thus,

$$V_\alpha = \sqrt{\frac{3}{2}}(q_1 - q_2)V_{dc} \tag{23}$$

$$V_\beta = \frac{1}{\sqrt{2}}(q_1 + q_2 - 1)V_{dc} \tag{24}$$

Let V_{ref} represents the reference voltage being synthesized by the 2L-4S inverter within a switching period of length. According to the space vector technique, the desired voltage can be mathematically expressed as:

$$V_{ref} = V_1 T_1 + V_2 T_2 + V_3 T_3 + V_4 T_4 \tag{25}$$

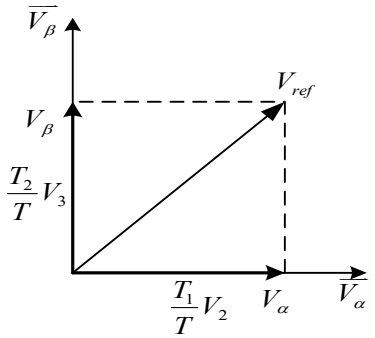

Fig. 5. Voltage vectors of the SVPWM in first section.

From Fig.5, T and V_{ref} in the section can be expressed as

$$V_{ref} = \frac{T_1}{T}V_1 + \frac{T_2}{T}V_2 = V_\alpha \alpha + V_\beta \beta \tag{26}$$

D. Modelling of SVPWM Control Patterns

Calculating the Section Data of V_{ref}

Using V_α and V_β, the angle and the corresponding section data of the desired voltage signal can be obtained.

$$\theta = \tan^{-1}\left(\frac{V_\beta}{V_\alpha}\right) \tag{27}$$

Calculating T_X, T_Y

The T_X, T_Y in Table 1can be calculated as follows. Section(1): 270~0 degrees.

From (23), (24), V_α and V_β can be calculated as expressed in (29).

$$V_1 = -\frac{1}{\sqrt{2}}V_{dc}\beta,\ V_2 = \sqrt{\frac{3}{2}}V_{dc}a \tag{28}$$

$$V_\alpha = \sqrt{\frac{3}{2}}V_{dc}\frac{T_2}{T},\ V_\beta = -\frac{1}{\sqrt{2}}V_{dc}\frac{T_1}{T} \tag{29}$$

Also, the T_1 and T_2 can be obtained as follows.

$$T_1 = -\sqrt{2}\frac{T}{V_{dc}}V_\beta,\ T_2 = -\sqrt{\frac{2}{3}}\frac{T}{V_{dc}}V_\alpha \tag{30}$$

$$T_X = \sqrt{2}\frac{T}{V_{dc}}V_\beta,\ T_Y = \sqrt{\frac{2}{3}}V_\alpha \tag{31}$$

With the similar method, the T_1 and T_2 in other sections can be readily derived.

Switch Sequences of the SVPWM

In normal operations, a triangle wave with proper frequency is used to compare with T_{aon}, T_{bon} and T_{con}. The amplitude of the triangle wave represents modulated period T while the frequency of the triangle wave can be chosen based on the capability of IGBT used.

Table 1. The T_1 and T_2 in all sections

Sections / Values	S1 270^0-0^0	S2 0^0-90^0	S3 90^0-180^0	S4 180^0-270^0
T_1	$-T_X$	$-T_X$	T_y	$-T_y$
T_2	$-T_Y$	T_Y	T_x	T_x

To make an easier representation of the PWM operations, two variables CMPR1 and CMPR2 can be used in section I to IV as shown in Table 2.

Table 2. The comparator values in various sections

Sections / Values	S1 270^0-0^0	S2 0^0-90^0	S3 90^0-180^0	S4 180^0-270^0
CMPR1	Tcon	Tbon	Taon	Tbon
CMPR2	Tbon	Tcon	Tbon	Taon

The corresponding PWM switching patterns in section I is shown in Fig. (6).

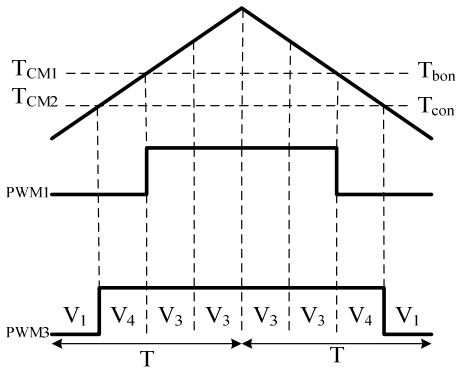

Fig. 6. The corresponding PWM switching patterns in section I.

III. Implementation of STATCOM P-Q Controllers

As mentioned previously, in a normal operation two sets of separate controllers are used for controlling the STATCOM, one for the real power (or equivalently the dc voltage) and the other for reactive power regulation. As well known, control of the STATCOM active and reactive currents can be achieved by respectively varying the active and reactive components of the internal inverter voltage. Fig. 7 shows the control system block diagram of the proposed P-Q controllers and the STATCOM circuits.

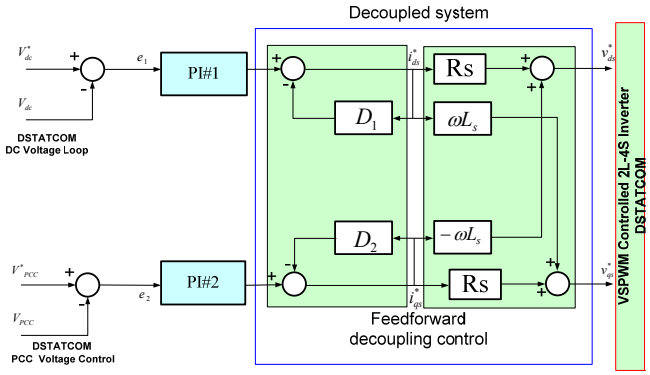

Fig. 7. The control system block diagram of the proposed P-Q controllers

IV. Test Power Systems and Results

For identifying and controlling the dynamics of the power system and the 2-leg 4-switch STATCOM, the single-machine infinite-bus (SMIB) power system as shown in Fig.8 is simulated in a Matlab/Simulink environment. Simulink model tool is a commercial grade transient simulator of electric networks with the capability of modeling complex power electronics, controls and the nonlinear power network. The power system shown in Fig. 8 comprises a voltage source (normally a synchronous generator with an automatic voltage regulator (AVR) is used), which is connected to a load bus through a transmission lines. The STATCOM is placed at the load bus to support the voltage. This simple system is chosen in order to evaluate the power flow control performances of the proposed new STATCOM configurations with two basic control strategies, i.e. reactive power and voltage regulations. The detailed control structure for the proposed STATCOM and the related system parameters can be found in Fig. 8. In Fig. 8, the control scheme shown in Fig. 7 (PI and decoupled controllers) is used to perform the P&Q power flow control functions. Fig. 9 to 10 show a set of typical simulation results obtained in this study. In Fig. 9 to 10, the control results concerning the real and reactive power regulations of a STATCOM are presented.

To demonstrate the performance of the proposed hardware simplified STATCOM in voltage regulation, Fig. 11 to Fig. 16 show a set of comparative simulation results concerning the PCC voltage regulations under load disturbances (two-steps in load changes) with the various switching methods working on both the 3-leg 6-switch and the 2-leg 4switch inverter topologies.

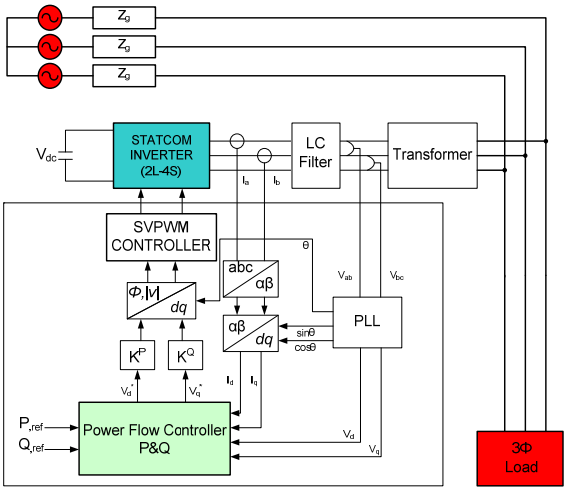

Fig. 8. The overall control system and parameters

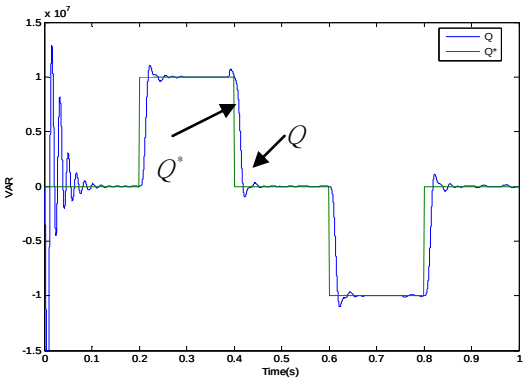

Fig. 9. (a) Reactive power regulations (two-steps in Q command changes) with the proposed SVPWM controller.

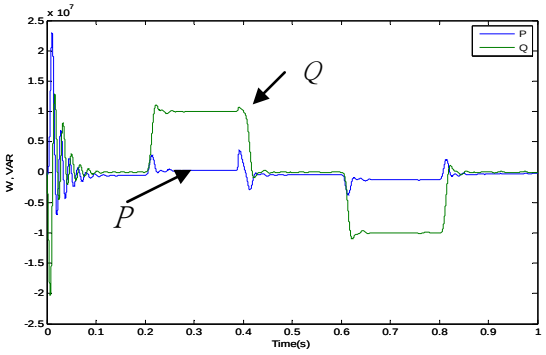

Fig. 9. (b) The effects of reactive power regulations (two-steps in Q command changes) on the real power (the blue line) with the proposed SVPWM controller.

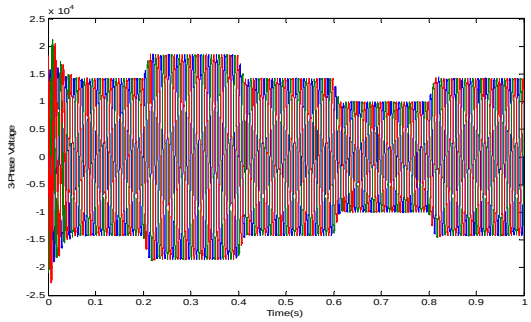

Fig. 9. (c) The terminal voltages of the STATCOM in reactive power regulations (two-steps in Q command changes) with the proposed SVPWM controller.

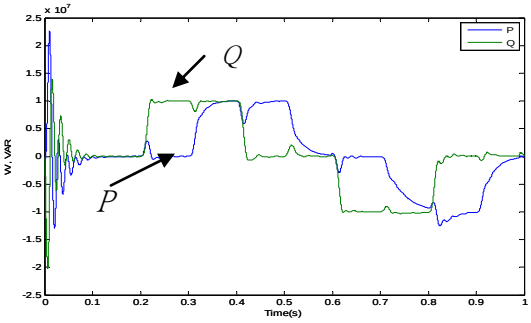

Fig. 10. (a) The P-Q regulation results (two-steps in P-Q command changes) with the proposed SVPWM controller (with a dc energy storage added).

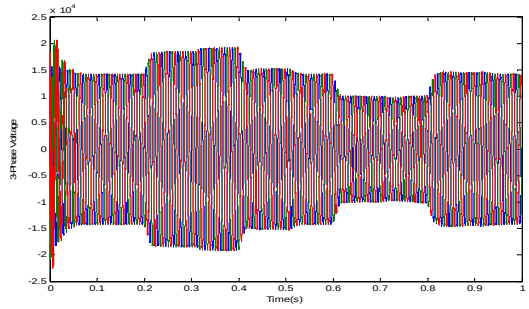

Fig. 10. (b) The terminal voltages of the STATCOM in P-Q regulations (two-steps in P-Q command changes) with the proposed SVPWM controller.

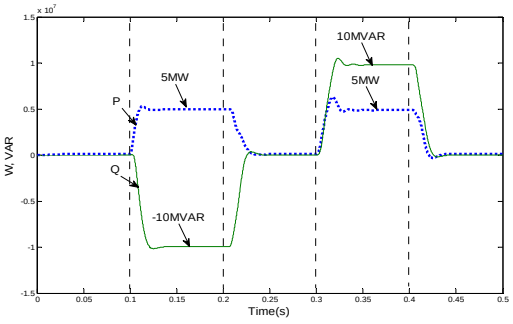

(A) The variations of P and Q.

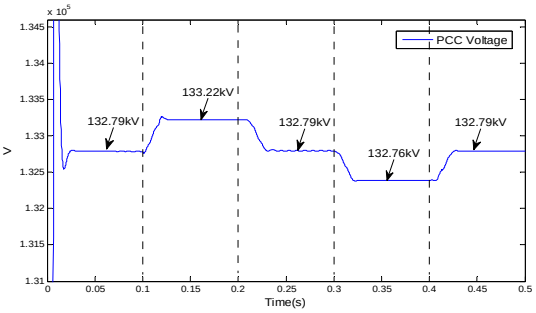

(B) PCC Voltage profile (uncontrolled)

Fig. 11. The initial system states with two-steps in load changes: (A) The variations of P and Q; (B) PCC Voltage profile (uncontrolled).

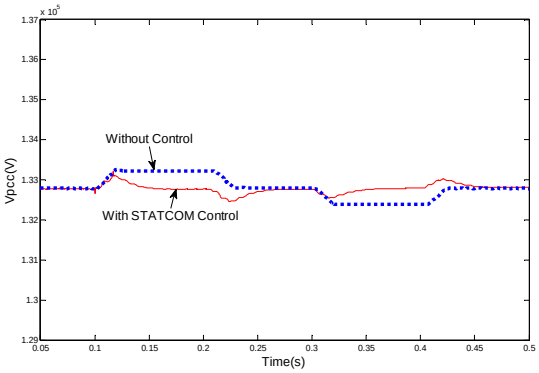

(A) The controlled Vpcc.

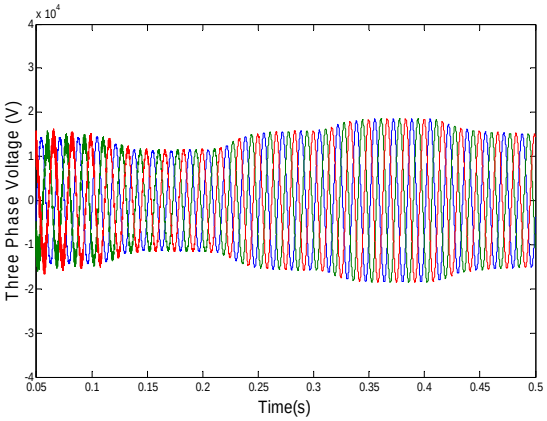

(B) The three-phase voltages of the STATCOM.

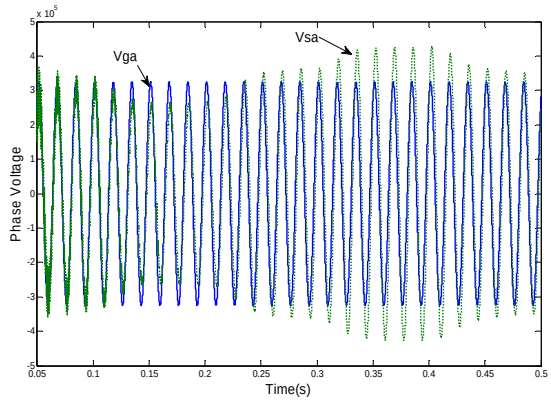

(C) The voltage difference between the grid and the STATCOM.

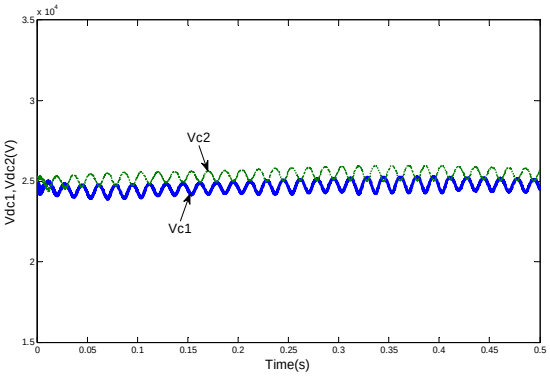

(D) The internal voltages on the two capacitors.

Fig. 12. The system states with the 2L-4S STATCOM in operation (SPWM control); (A) the controlled Vpcc, (B) The three-phase voltages of the STATCOM; (C) The voltage difference between the grid and the STATCOM; (D) The internal voltages on the two capacitors.

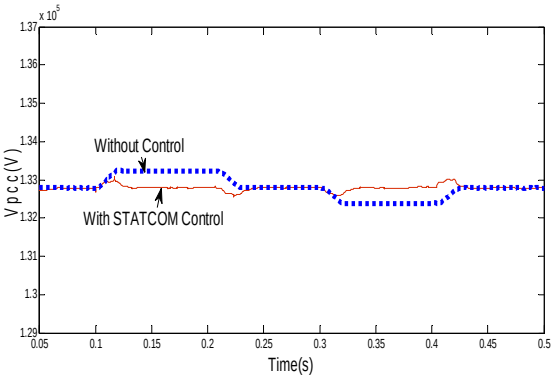

(A) The controlled Vpcc.

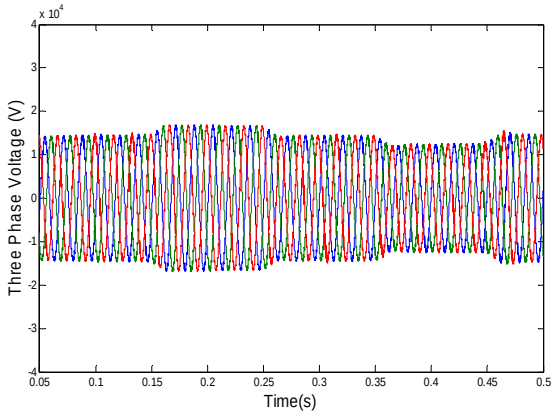

(B) The three-phase voltages of the STATCOM.

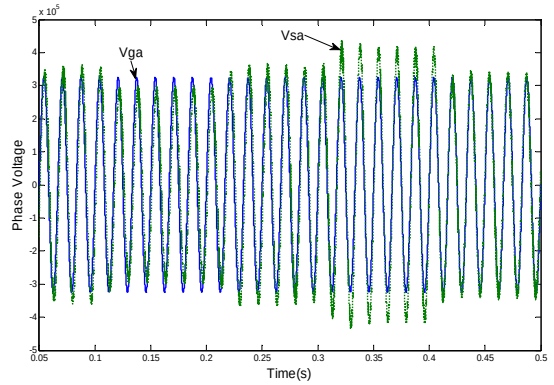

(C) The voltage difference between the grid and the STATCOM.

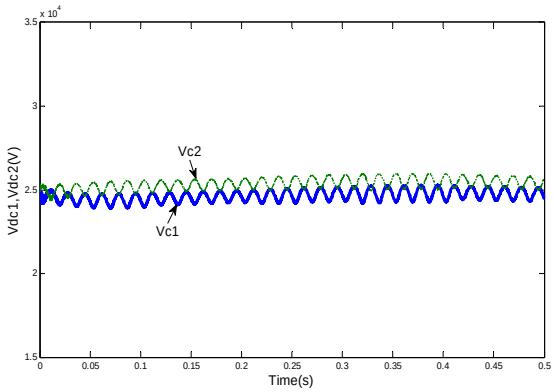

(D) The internal voltages on the two capacitors.

Fig. 13. The system states with the 2L-4S STATCOM in operation (Hysteresis control); (A) the controlled Vpcc, (B) The three-phase voltages of the STATCOM; (C) The voltage difference between the grid and the STATCOM; (D) The internal voltages on the two capacitors.

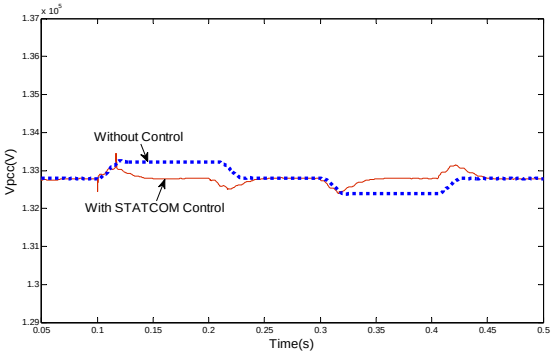

(A) The controlled Vpcc.

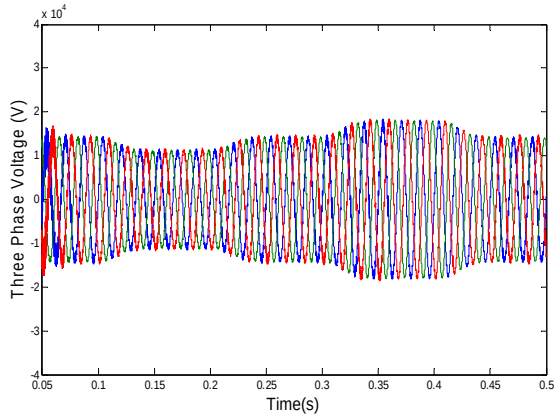

(B) The three-phase voltages of the STATCOM.

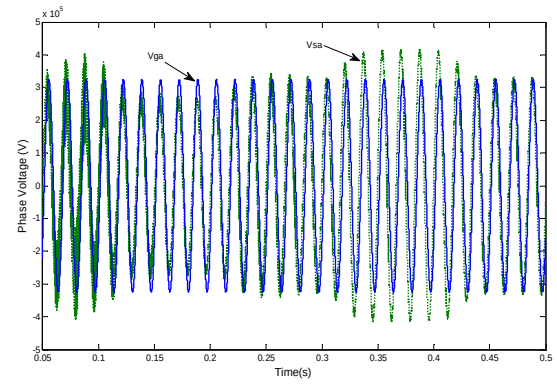

(C) The voltage difference between the grid and the STATCOM.

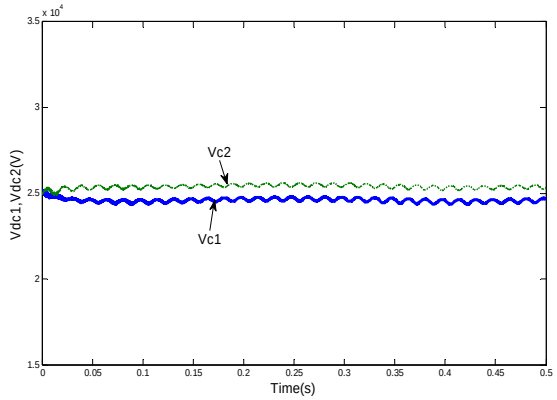

(D) The internal voltages on the two capacitors.

Fig. 14. The system states with the 2L-4S STATCOM in operation (SVPWM control); (A) the controlled Vpcc, (B) The three-phase voltages of the STATCOM; (C) The voltage difference between the grid and the STATCOM; (D) The internal voltages on the two capacitors.

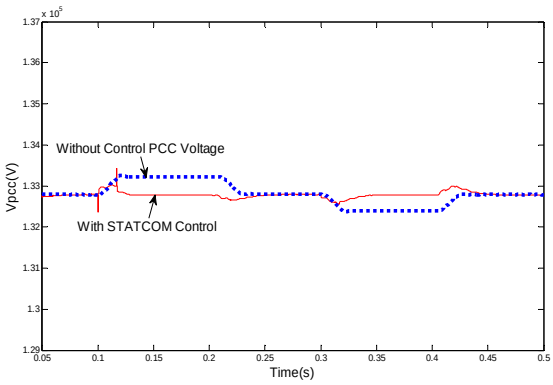

(A) The controlled Vpcc.

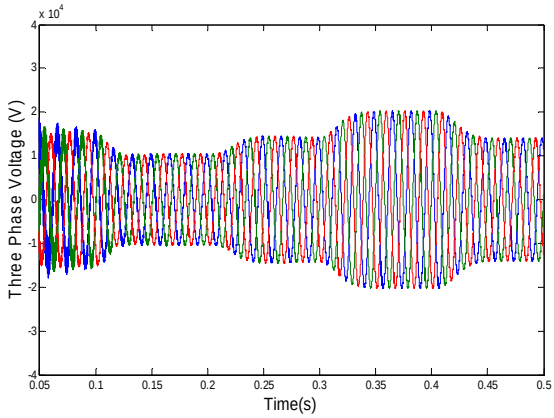

(B) The three-phase voltages of the STATCOM.

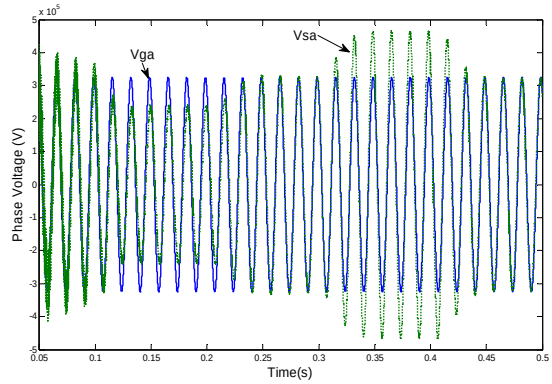

(C) The voltage difference between the grid and the STATCOM.

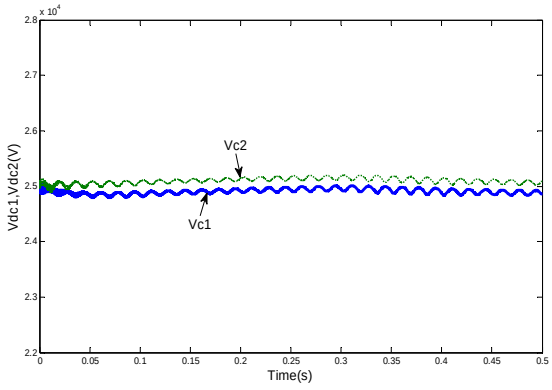

(D) The internal voltages on the two capacitors.

Fig. 15. The system states with the 2L-4S STATCOM in operation (3L-6S, SVPWM control); (A) the controlled Vpcc, (B) The three-phase voltages of the STATCOM; (C) The voltage difference between the grid and the STATCOM; (D) Internal voltages on the two capacitors.

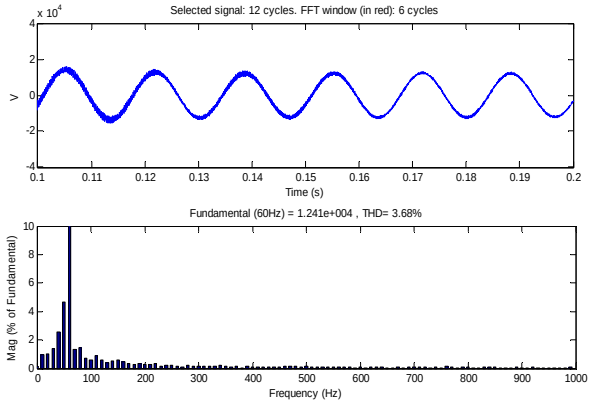

(A) The SPWM controlled 2L-4S STATCOM.

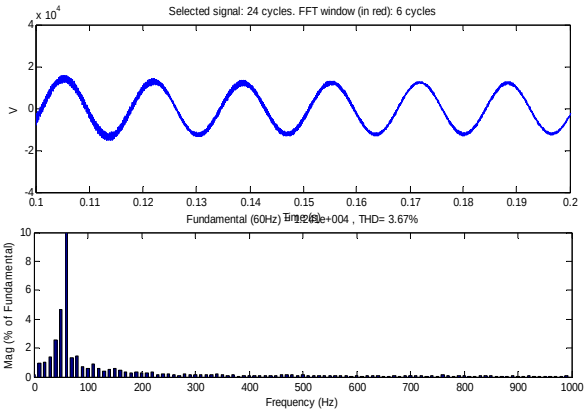

(B) The voltage hysteresis controlled 2L-4S STATCOM.

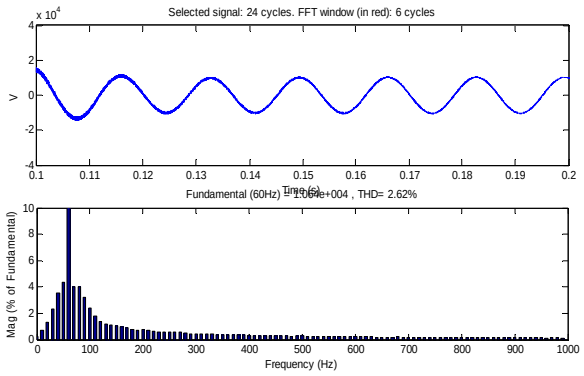

(C) The SVPWM controlled 2L-4S STATCOM.

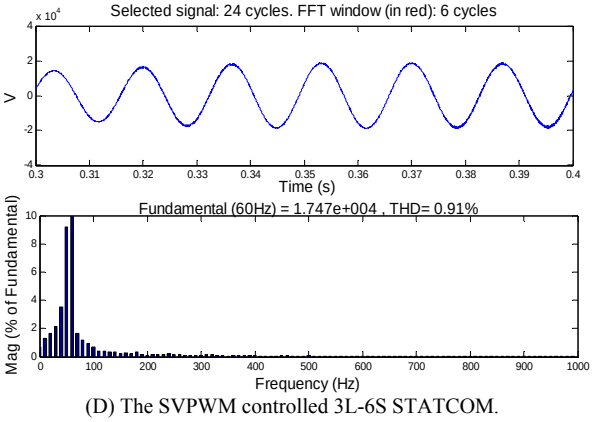

(D) The SVPWM controlled 3L-6S STATCOM.

Fig. 16. The spectra of voltage harmonics of the 2L-4S STATCOM under different switching control strategies: (A) The SPWM controlled STATCOM, (B) The voltage hysteresis controlled STATCOM; (C) The SVPWM controlled STATCOM; (D) The 3L-6S Inverter based STATCOM with SVPWM control.

V. Conclusion

This paper has presented both the theoretical and numerical investigations on a hardware simplified STATCOM based on a two-leg four-switch inverter. The proposed STATCOM is designed to provide satisfactory performances in performing various reactive power flow regulation functions during steady-state and dynamic voltage control of power systems. To verify the overall performance of the designed STATCOM, two topologies, i.e. 2L-4S and 3L-6S with three switching techniques, i.e. SPWM, voltage hysteresis and SVPWM, have been investigated. Based on comprehansive simulation studies carried out in this study, the proposed inverter circuit with SVPWM switching strategy exibits a number of good features in that it can fast modify the switching patterns of the internal power electronic switches of the STATCOM to achieve the desired output voltage with only 2 thirds of the number of power devices required in a conventional design. This paper has also developed a detailed dynamic model of the proposed 2L-4S STATCOM in d-q frame. The derived model has been verified with a practical design case in which the basic P-Q power flow control and voltage stabilization functions in a STATCOM are tested. Feasibility and control performance of the new STATCOM system, including the simplified power circuitry and control subsystems have been verified via comprehensive digital time-domain simulations. Results have shown the feasibility and effectiveness of the design.

References

[1] A. Lotfjou, M. Shahidehpour, Fu Yong and Li Zuyi, "Security-Constrained Unit Commitment With AC/DC Transmission Systems," *IEEE Transactions on Power Systems, Volume: 25 , Issue: 1* , pp. 531 – 542, 2010.

[2] M. Zarghami, M.L. Crow and S. Jagannathan, "Nonlinear Control of FACTS Controllers for Damping Interarea Oscillations in Power Systems," *IEEE Transactions on Power Delivery, Volume: 25 , Issue: 4* , pp. 3113-3121, 2010.

[3] X. gping and S. Bhattacharya, "Performance improved during system fault of angle controlled STATCOM by current control," *IEEE Power and Energy Society General Meeting*, pp. 1 – 8, 20-24 July 2008.

[4] K. Li, J. Liu , Z. Wang and B. Wei, "Strategies and Operating Point Optimization of STATCOM Control for Voltage Unbalance Mitigation in Three-Phase Three-Wire Systems," *IEEE Trans. PD*, *Vol. 22*, *Issue 1*, pp. 413 – 422, Jan. 2007.

[5] X. Zhengping and S. Bhattacharya, "STATCOM Control and Operation with Series Connected Transformer Based 48-pulse VSC," *IEEE Industrial Electronics Conference*, pp. 1714 – 1719, Nov. 2007.

[6] Tsao-Tsung Ma, "New Control Strategies for a Two-Leg Four-Switch STATCOM," Lecture Notes in Engineering and Computer Science: Proceedings of The International MultiConference of Engineers and Computer Scientists 2011, IMECS 2011, 16-18 March, 2011, Hong Kung, pp927-932.

[7] S. Qiang, L. Wenhua and Y. Zhichang, "Multilevel Optimal Modulation and Dynamic Control Strategies for STATCOMs Using Cascaded Multilevel Inverters," *IEEE Transactions on Power Delivery*, *vol 22*, *no 3*, pp.1937 – 1946, July 2007.

[8] H. Xie, L. Angquist and H.-P. Nee, "Comparison of Voltage and Flux Modulation Schemes of StatCom Regarding Transformer Saturation During Fault Recovery," *IEEE Transactions on Power Systems*, *vol 23*, *no 4*, pp.1653 – 1661, Nov. 2008.

[9] R. Sternberger and D. Jovcic, "Theoretical Framework for Minimizing Converter Losses and Harmonics in a Multilevel STATCOM," *IEEE Transactions on Power Delivery*, *vol 23*, *no 4*, pp.2376 – 2384, Oct. 2008.

[10] G. Zhao, J. Liu and Z. Wang, "An analysis on the influence of interface inductor to STATCOM system with phase-shift control and corresponding design considerations," *IEEE Conference on Power Electronics and Motion Control,* pp.2339 – 2344, May 2009.

[11] S. Mohagheghi, G.K. Venayagamoorthy, S. Rajagopalan and R.G. Harley, "Hardware Implementation of a Mamdani Fuzzy Logic Controller for a Static Compensator in a Multimachine Power System," *IEEE Transactions on Industry Applications*, *vol 45*, *no 4*, pp.1535 – 1544, July-aug. 2009.

[12] N. oraphonpiput and S. Chatratana, "STATCOM Analysis and Controller Design for Power System Voltage Regulation," *IEEE/PES 2005 Transmission and Distribution Conference and Exhibition*, pp. 1 – 6, July 2005.

[13] V. Spitsa, A. Alexandrovitz and E. Zeheb, "Design of a Robust State Feedback Controller for a STATCOM Using a Zero Set Concept," *IEEE Transactions on Power Delivery*, *vol 25*, *no 1*, pp.456 – 467, Jan. 2010.

[14] B. Singh, S.S. Murthy and S. Gupta, "STATCOM-Based Voltage Regulator for Self-Excited Induction Generator Feeding Nonlinear Loads," *IEEE Transactions on Industrial Electronics*, *vol 53*, *no 5*, pp.1437 – 1452, Oct. 2006.

[15] B. Singh, S.S. Murthy and S. Gupta, "Analysis and design of STATCOM-based voltage regulator for self-excited induction generators," *IEEE Transaction on Energy Conversion*, *vol 19*, *no 4*, pp.783 – 790, Dec. 2004.

[16] J.A. Suul, M. Molinas and T. Undeland, "STATCOM-Based Indirect Torque Control of Induction Machines During Voltage Recovery After Grid Faults," *IEEE Transactions on Power Electronics, Volume: 25 , Issue: 5*, pp. 1240 – 1250, 2010.

[17] Song. Wenchao and A.Q. Huang, "Fault-Tolerant Design and Control Strategy for Cascaded H-Bridge Multilevel Converter-Based STATCOM," *IEEE Transactions on Industrial Electronics, Volume: 57 , Issue: 8*, pp. 2700 – 2708, 2010.

[18] Woei-Luen Chen, Wei-Gang Liang and Hrong-Sheng Gau, "Design of a Mode Decoupling STATCOM for Voltage Control of Wind-Driven Induction Generator Systems," *IEEE Transactions on Power Delivery, Volume: 25 , Issue: 3,* pp. 1758 – 1767, 2010.

[19] N. Hatano and T. Ise, "Control Scheme of Cascaded H-Bridge STATCOM Using Zero-Sequence Voltage and Negative-Sequence Current," *IEEE Transactions on Power Electronics, Volume: 25 , Issue: 2*, pp. 543 – 550, 2010.

[20] Q. Wei, R.G. Harley and G.K. Venayagamoorthy, "Coordinated Reactive Power Control of a Large Wind Farm and a STATCOM Using Heuristic Dynamic Programming," *IEEE Transactions on Energy Conversion*, *vol 24*, *no 2*, pp.493 – 503, June 2009.

[21] T.T. Ma, "Space Vector Model and Control of a Two-Leg Four-Switch STATCOM," *IREE, Part-A, vol. 5. n.3*, pp. 900-908, 2010.

[22] G. Shahgholian, "Development of State Space Model and Control of the STATCOM for Improvement of Damping in a Single-Machine Infinite-Bus," *IREE, Part-B, vol. 4. n. 6*, pp. 1367-1375*,* 2009.

[23] H. Xie, L. Angquist and H.-P. Nee, "Design and Analysis of a Controller for a Converter Interface Interconnecting an Energy Storage With the DC Link of a VSC," *IEEE Transactions on Power Systems, accepted for future publication*, pp.1 – 9, 2009.

[24] H. Gaztanaga, I. Etxeberria-Otadui, D. Ocnasu and S. Bacha, "Real-Time Analysis of the Transient Response Improvement of Fixed-Speed Wind Farms by Using a Reduced-Scale STATCOM Prototype," *IEEE Transactions on Power Systems*, *vol 22*, *no 2*, pp.658 – 666, May 2007.

[25] C.-H. Liu and Y.-Y. Hsu, "Design of a Self-Tuning PI Controller for a STATCOM Using Particle Swarm Optimization," *IEEE Transactions on Industrial Electronics*, *vol 57,* pp. 702-715, 2010.